Structure *14*, 837–845, May 2006 ©2006 Elsevier Ltd All rights reserved DOI 10.1016/j.str.2006.03.010

Highly Discriminatory Binding of Capsid-Cementing Proteins in Bacteriophage L

Liang Tang,[1,3] Eddie B. Gilcrease,[2] Sherwood R. Casjens,[2] and John E. Johnson[1,*]
[1]Department of Molecular Biology
The Scripps Research Institute
10550 North Torrey Pines Road
La Jolla, California 92037
[2]Division of Cell Biology and Immunology
Department of Pathology
University of Utah Medical School
Salt Lake City, Utah 84132
[3]Department of Molecular Biosciences
University of Kansas
Lawrence, Kansas 66045

Summary

Cementing proteins that bind to the virion surface have been described in double-stranded DNA viruses such as herpesvirus, adenovirus, and numerous bacteriophages. The three-dimensional structure of bacteriophage L determined by electron cryo-microscopy reveals binding modes of two cementing proteins—one, called Dec, encoded by phage gene *orf134* and the other by an as yet unidentified gene. These two proteins form homotrimers and bind at the quasi 3-fold axes nearest the icosahedral 2-fold axes and at the icosahedral 3-fold vertices, respectively. They do not bind at the quasi 3-fold axes near the icosahedral 5-fold vertices. These observations indicate precise recognition of the two cementing proteins at a subset of the quasi equivalent sites on the phage capsid. Sequence analysis shows striking similarity between the C-terminal portion of phage L Dec protein and five regions in the long tail fiber of a T4-like phage, suggesting functional parallelism between them.

Introduction

A common feature of the assembly of many large and complex virus particles is the presence of proteins that embellish the structures built by the basic virion building block proteins such as the icosahedrally arranged coat protein. Among these embellishments are proteins that "decorate" the exterior of capsids (Casjens and Hendrix, 1988). They usually do not have a form-determining role, and they bind to the virion's exterior only after the shell itself has assembled. Some decoration proteins stabilize the capsid, and those that do so have been called "glue" or "cementing" proteins since they give the shell increased physical strength and/or stability (Furcinitti et al., 1989; Stewart et al., 1991). These are usually small to mid-size proteins that bind at specific sites on the virus surface. They are sometimes considered to have "accessory" functions since they are often not essential to virion formation or the virus lifecycle and may not be present in all members of a group of closely related viruses. In eukaryotic viruses, where the capsid is internalized into the infected cell, decoration proteins may have additional functions within the cell. Finally, because of their exposed location, their ability to be genetically manipulated, and their many copies per virion, the decoration proteins of phage lambda and adenovirus have been engineered as protein display systems (Gupta et al., 2003; Meulenbroek et al., 2004; Mikawa et al., 1996; Zakhartchouk et al., 2004).

Decoration proteins have been described and studied in eukaryotic viruses such as adenovirus and herpesvirus and in the tailed bacterial viruses such as T4 and lambda. In T4, two decoration proteins, Hoc and Soc, were the first such proteins to be characterized. Soc protein binds between coat protein hexons and increases the stability of the prolate T = 13 phage head against extremes of pH and temperature, whereas protein Hoc binds at the center of each hexon and has only a marginal effect on the head stability under the conditions tested (Fokine et al., 2004; Ishii and Yanagida, 1977; Iwasaki et al., 2000; Steven et al., 1992). It is interesting to note that Hoc and Soc proteins are not encoded by all close relatives of T4 (Yanagida, 1977; Yanagida et al., 1984). The protein gpD in phage lambda occupies all of the interhexamer and pentamer 3-fold sites on the capsid lattice, so there are equal numbers of coat and gpD molecules in the phage head (Casjens and Hendrix, 1974; Dokland and Murialdo, 1993; Imber et al., 1980). Wild-type lambda heads are very unstable without gpD, and so it is considered to be essential for virion production; however, gpD becomes dispensable if shorter chromosomes are packaged (Sternberg and Weisberg, 1977; Wendt and Feiss, 2004). Thus, gpD appears to stabilize the icosahedral head shell against internal "DNA pressure." Phage ϕ29 also carries a decoration protein that is highly elongated and extends as a fiber outward from each of the quasi 3-fold sites on its prolate T = 3 head that are adjacent to a 5-fold axis (Morais et al., 2005; Tao et al., 1998); it is not known if it stabilizes the capsid. The T = 25 lipid-containing phage PRD1 may also have decoration proteins, but they have not been studied in detail (San Martin et al., 2002). In the adenoviruses, polypeptides pIIIa and pIX bind between the coat protein hexons in which pIX has been shown to stabilize the T = 25 capsid (Fabry et al., 2005; Furcinitti et al., 1989; Rux and Burnett, 2004; Stewart et al., 1991; Vellinga et al., 2005). In addition, pIX has other roles in virus proliferation and interference of host cell antiviral activity (Lutz et al., 1997; Rosa-Calatrava et al., 2001). Like lambda gpD, adenovirus pIX is dispensable for virion assembly if a shorter than normal chromosome is packaged (Sargent et al., 2004). In α-herpesviruses such as herpes simplex virus 1, the heterotrimeric "triplex," which contains two copies of VP23 and one copy of VP19c, binds between hexons (Newcomb et al., 1993; Spencer et al., 1998). Unlike the other decoration proteins mentioned here, the triplex is essential for assembly of the T = 16 capsid (Saad et al., 1999). The herpesvirus VP26, on the other hand, is not essential for shell assembly, binds to the exterior of

*Correspondence: jackj@scripps.edu

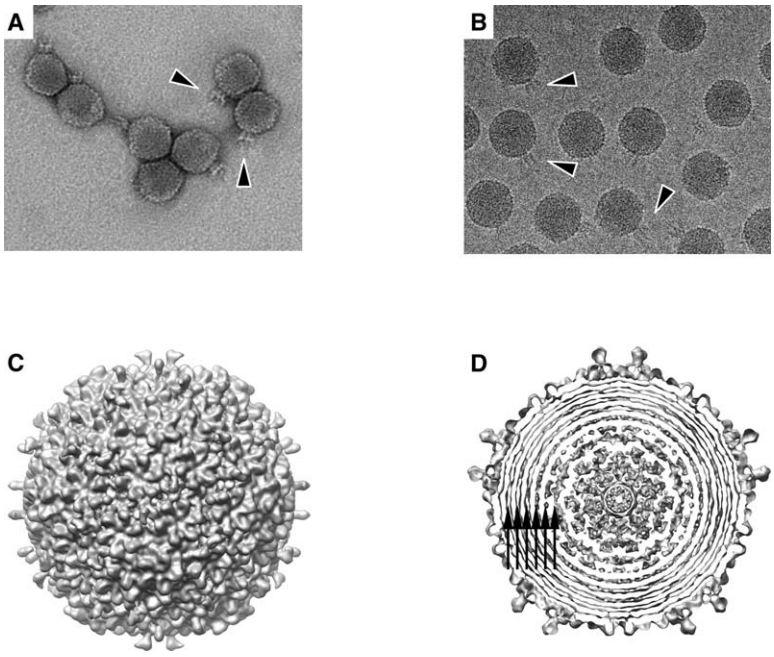

Figure 1. The Structure of Phage L

(A) Electron micrograph of phage L negatively stained with uranyl acetate.

(B) Electron micrograph of frozen-hydrated phage L. Arrowheads indicate the tail structure of phage L.

(C) Isosurface of the cryo-EM map of phage L viewed down an icosahedral 2-fold axis.

(D) A 30 Å thick cross-section of the phage L map viewed down the icosahedral 5-fold axis. The outer layer of density corresponds to the protein capsid. The concentric layers of density for the packaged DNA genome inside the capsid are indicated by arrows.

coat protein hexamers after shell assembly, and serves to attach capsids to dynein motors for transport to the nucleus in the infected cell (Douglas et al., 2004; Newcomb et al., 2000; Trus et al., 1995; Zhou et al., 1995).

Bacteriophage L is a short-tailed dsDNA bacteriophage with a virion chromosome that is 43.4 kbp in length (Hayden et al., 1985), and it is a close relative of well-studied model system phage P22 (Prevelige, 2005). Previous work pointed to the presence of a decoration/cementing protein, called Dec, encoded by phage L *orf134* that stabilizes virions substantially against heat and divalent cation chelator treatment (Gilcrease et al., 2005). Here, we report the three-dimensional structure of phage L virions and the structure of P22 virions decorated with Dec protein, determined by electron cryomicroscopy (cryo-EM) and image reconstruction. To our knowledge, these structures reveal novel binding modes of the cementing proteins in phage L. Dec protein binds in a trimeric form at the quasi 3-fold axes nearest the icosahedral 2-fold axes. We have also identified a putative second decoration protein, encoded by an as yet unidentified phage L gene, that occupies the virion's icosahedral 3-fold vertices. An analysis of these two binding sites indicates precise recognition by each of these two proteins of only a subset of quasi equivalent sites on the surface of the phage capsid.

Results and Discussion

The Three-Dimensional Structure of Bacteriophage L Virions

The three-dimensional structure of phage L was determined at 15 Å resolution by cryo-EM and image reconstruction. A total of 5581 images of frozen-hydrated phage particles from 13 electron micrographs were used in the calculation. Each phage contains a short-tail complex situated at a single vertex of the phage head, as observed both in the negatively stained EM images and in cryo-EM images (Figures 1A and 1B). Because icosahedral symmetry was imposed in the calculation, the tail is not visible in the reconstruction.

The phage L capsid is an isometric icosahedral lattice with a diameter of ~650 Å between 5-fold vertices (Figure 1C). The structure shows discernible features and protruding domains on the surface that allow for straightforward determination of the icosahedral lattice of phage L virions as T = 7 *laevo*, the same as previously determined for its close relative phage P22 (Casjens, 1979; Prasad et al., 1993). The icosahedral asymmetric unit is made up of a hexamer of subunits plus one subunit of the pentamer at the 5-fold vertex. A section through the center of the phage L cryo-EM map shows up to six concentric thin layers of density underneath the capsid protein density and a distance of ~25 Å between adjacent layers (Figure 1D). Similar concentric layers of density have been observed in the cryo-EM structures of other large dsDNA viruses, such as herpesviruses (Booy et al., 1991; Zhou et al., 1999), and other tailed phages (Cerritelli et al., 1997; Fokine et al., 2004, 2005; Zhang et al., 2000) and are almost certainly due to the icosahedrally averaged image of the packaged DNA. Low-angle X-ray diffraction data from the closely related phage P22 strongly supported this view (Earnshaw et al., 1976; Earnshaw and Harrison, 1977).

Structure and Location of Phage L Decoration/Cementing Proteins

When the icosahedral shell of the phage L virion is compared to that of phage P22 (the latter as previously determined by Zhang et al. [2000], as well as by ourselves in this study; Figure 2A), it can be seen that the two coat protein shells are very similar. This is as expected since their coat protein sequences are extremely similar (see below). However, there is substantial extra density in the phage L map protruding outward from the surface at the quasi 3-fold axes nearest the icosahedral 2-fold

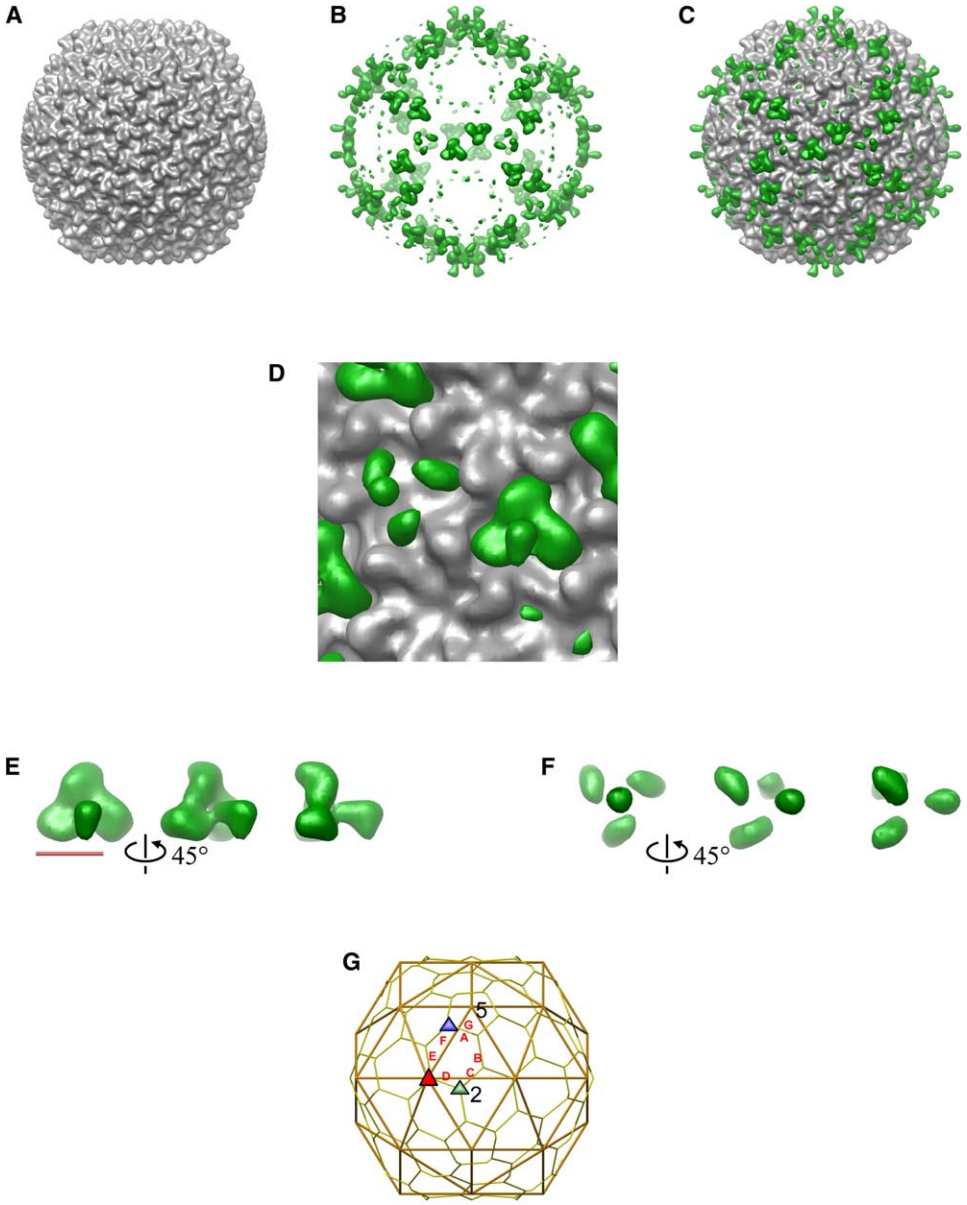

Figure 2. The Structures of the Cementing Proteins in Phage L

(A) The cryo-EM map of the wild-type phage P22.

(B) The difference map between phages L and P22.

(C) The difference map between phages L and P22 (green) superimposed with the phage P22 map (gray).

(D) Close-up of the two binding sites of phage L cementing proteins (green) superimposed with the phage P22 map (gray).

(E) Views of isolated density of the cementing (Dec) protein that binds at the quasi 3-fold axis nearest the icosahedral 2-fold axis. The scale bar indicates 50 Å.

(F) Views of isolated density of the cementing protein that binds at the icosahedral 3-fold axis. The scale is the same as in (E).

(G) A schematic diagram of the T = 7 *laevo* icosahedral lattice. The T = 7 hexagonal lattice and the icosahedral lattice are shown as yellow and gold sticks, respectively. The positions of the seven coat protein subunits in an icosahedral asymmetric unit are indicated with (A)–(G). Subunit G participates in the formation of a pentamer at the icosahedral 5-fold axis, and subunits A–F form a hexamer. The two quasi equivalent, local 3-fold sites are labeled with a green (nearest the icosahedral 2-fold axis) and blue (near the icosahedral 5-fold axis) triangle, respectively. The icosahedral or true 3-fold axis is indicated with a red triangle. The icosahedral 5- and 2-fold axes are indicated by numbers.

axes and at the icosahedral 3-fold axes. This can be seen in a difference map between phage L and phage P22 virions (Figure 2B; see Figure 2G for a schematic diagram of the T = 7 *laevo* icosahedral lattice). At both sites, this extra density in phage L is tripod shaped, with a "head" at the top and three "legs" extending down toward the coat protein shell's surface. We believe that each of these tripod units is formed by a protein trimer since they each have clear 3-fold symmetry. At least the majority of this density is likely due to the phage L Dec protein, which we have previously shown to bind to the outside of phage L in large numbers and to exist as a trimer in its assembly-active solution form (Gilcrease et al., 2005). It is simplest to imagine that the

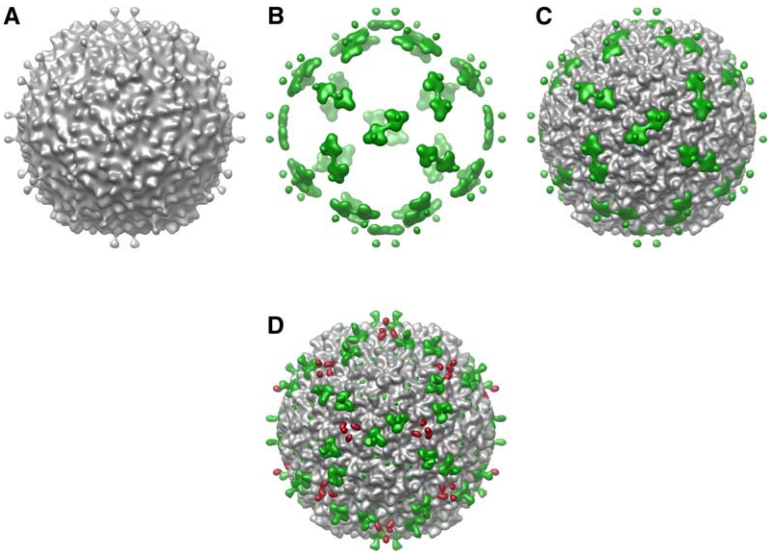

Figure 3. The Structure of Phage P22 Decorated with the Phage L Cementing Protein Dec

(A) The cryo-EM map of phage P22 with Dec protein.

(B) The difference map between phage P22 with Dec protein and wild-type phage P22.

(C) The difference map (green) superimposed with the phage P22 map (gray).

(D) The segmented cryo-EM structure of the phage L virion. The gray isosurface corresponds to the major capsid that is similar to that of the phage P22 virion. The densities for the Dec protein (at quasi 3-fold axes, see text) and the second decoration protein (at the icosahedral 3-fold axes) deduced from the difference map between phages L and P22 (Figure 2B) are colored green and red, respectively. The tiny density colored in green surrounding the 5-fold axes is likely noise in the difference map.

monomers within the tripod are each composed of a head domain and a leg domain. The head domain is responsible for trimerization, whereas the leg domain binds the phage capsid. Although the head domain appears to be disconnected from the leg domains in the tripod density at the icosahedral 3-fold axis (Figures 2B, 2D, and 2F), they are connected if the map is contoured at a slightly lower level, suggesting a slender linkage between the two domains. The bulk of all of the tripod densities is situated a short distance above the capsid, therefore creating hollow space between them and the capsid; the leg domains interact with surface protrusions of the coat proteins.

We note that the tripods appear to make contact with the major capsid proteins in two different ways (Figures 2C and 2D). Each tripod at the quasi 3-fold axis nearest the icosahedral 2-fold axis has a greater area of contact with the six coat protein subunits surrounding it, although this interface is not 6-fold symmetric. On the other hand, the tripod at the icosahedral 3-fold site appears to interact with only three of the six adjacent coat protein subunits. This difference in contact with the capsid might result from the different structures of the proteins that occupied these two sites and/or different occupancy (see below). Interestingly, although the density that binds to the quasi 3-fold sites is apparently trimeric in its leg domains, its head domains showed features that deviate from a perfect trimeric conformation (Figures 2D and 2E). This is reminiscent of the heterotrimeric triplex proteins in herpes simplex virus that are composed of two copies of VP23 and one copy of VP19c. The functional implication of this discrepancy from true 3-fold symmetry is unclear.

The Dec Protein Binds at the Equivalent Sites on Phage P22

We incubated purified phage L Dec protein expressed in *E. coli* with purified P22 virions, repurified the virions with Dec bound, and conducted a cryo-EM reconstruction of the resulting particles. The map showed extra density only at the quasi 3-fold sites nearest the icosahedral 2-fold axis (Figures 3A–3C); no extra density was seen at the icosahedral 3-fold axes. The shape of this extra density, and its contact with the capsid, very closely resembles that in the phage L map. Therefore, we conclude that the density at these quasi 3-fold sites in the phage L map is formed by Dec protein (Figures 2C and 3C).

The genetic origin of the putative phage L-encoded protein that forms the virion surface density at the icosahedral 3-fold axes remains unclear. It must be due either to Dec protein that binds at this position on L virions, but not on P22 virions, or to a different decoration protein that binds specifically to the icosahedral 3-fold site. We favor the later explanation for two reasons. First, the shape and contact position on the coat protein of the trimeric densities at the icosahedral 3-fold sites are clearly different from those of the other trimeric density (see above). It seems unlikely that the same protein (Dec) could be responsible for these different structures. Second, phage L and P22 coat proteins have only 4 rather conservative differences out of 430 amino acids: R101H, I154L, M267L, and A276T (P22 residue-residue number-phage L residue). Little is known about the details of P22 or L coat protein tertiary structure, so the spatial position of these differences is also unknown (see, for example, Kang and Prevelige, 2005). Nonetheless, it seems unlikely that such apparently minor differences (even if they were at the surface) could be responsible for Dec binding at the icosahedral 3-fold position of phage L virions. In addition, it seems even more unlikely that binding to such subtly different sites could cause the shape differences in Dec protein that would have to occur at the two different binding sites if it were responsible for the density at both sites. We therefore believe that a second decoration protein (not Dec protein) is bound to its icosahedral 3-fold locations. These deduced locations of the two different decoration proteins on the surface of the phage L virions are shown in Figure 3D. Since genes are usually clustered by function on phage genomes, it is possible that either phage L *orf118* or *orf129* (two genes of unknown function) might encode this protein, since they lie adjacent to the *dec* gene on the L genome (Gilcrease et al., 2005; Mmolawa

et al., 2003). Since there are 3 Dec molecules at each of the 60 equivalent quasi 3-folds nearest the icosahedral 2-fold axes, there are 180 molecules of Dec protein per phage L virion. This number is in excellent agreement with the experimentally measured values of 150 ± 30 for phage L virions and 185 ± 20 for Dec bound to P22 virions (Gilcrease et al., 2005). There are 60 molecules of the second decoration protein present as a trimer at each of the 20 equivalent icosahedral 3-fold locations.

The Phage L Decoration Proteins Are Capable of Distinguishing the Icosahedral and Quasi 3-Fold Sites

The quasi equivalence principle describes the geometrical architecture of capsids of icosahedral viruses (Caspar and Klug, 1962). The coat protein subunit arrangement is typically composed of pentamers at the 5-fold vertices and hexamers distributed according to the surface lattice T number. In the T = 7 structure observed in phages L and P22, there are true (icosahedral) 3-fold symmetry axes relating three hexamers at the face centers, as well as two independent locations with quasi 3-fold symmetry—one among three hexamers near the 2-fold axes and one among two hexamers and a pentamer near the 5-fold axes. The former two sites were discussed above; all three sites are quasi equivalently related to one another (Figures 2G and 4). The local environments of the three quasi equivalently related 3-fold sites are subtly different, although they are surrounded by chemically identical capsid protein components. According to the above discussion, phage L Dec protein occupies the quasi 3-fold sites near the 2-fold axes, the other decoration protein occupies the true 3-fold site, and neither binds to the quasi 3-fold site that lies between a coat pentamer and two hexamers. Thus, both decoration proteins are able to discriminate among the several quasi equivalently related binding sites.

We used the X-ray structure of the capsid of HK97 (Wikoff et al., 2000), another T = 7 dsDNA bacteriophage whose coat protein fold appears to be similar to that of the phage P22 coat (Jiang et al., 2003) and therefore to the phage L coat, as a model to investigate potential differences between the local environments surrounding the three quasi equivalently related decoration protein binding sites. Each of these HK97 3-fold sites is surrounded by not three, but nine coat protein subunits, considering the contribution of the extended N arms and E loops (Figures 4A and 4B). The coordinates of the nine subunits surrounding each quasi 3-fold site were superimposed onto those around the icosahedral 3-fold site, respectively, and yielded root-mean-square deviations (rmsds) in Cα of 4.19 Å between the icosahedral 3-fold and the quasi 3-fold nearest the icosahedral 2-fold, and 7.01 Å between the icosahedral 3-fold and the quasi 3-fold nearest the icosahedral 5-fold. If we superimposed only those residues within the reach of two cementing proteins (within 40 Å radius from the center of each protein), the Cα rmsds were 1.13 and 4.50 Å, respectively. The former was close to the Cα rmsd for superimposition between monomers within the canonical hexon, which was ~0.84 Å. Thus, the local structural environment of the icosahedral 3-fold site in phage L is likely to be very similar to that of the quasi 3-fold near the icosahedral 2-fold, although it is quite different

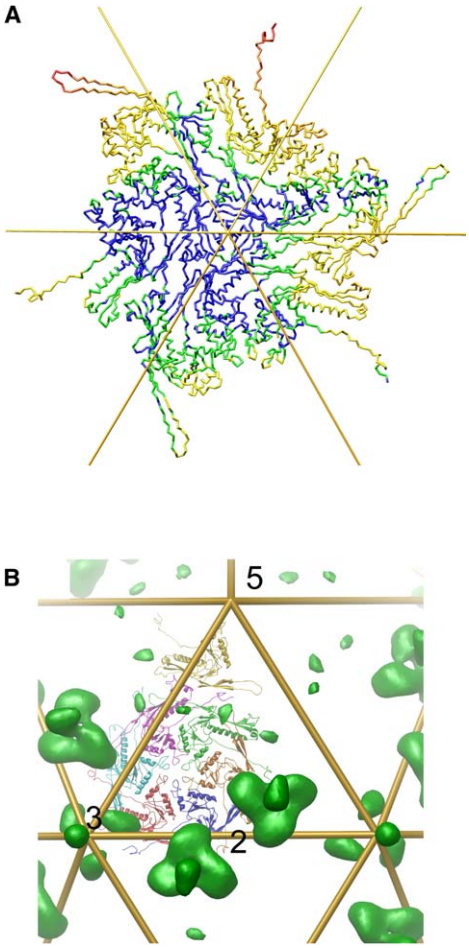

Figure 4. The Quasi Equivalent 3-Fold Sites

(A) The nine coat protein subunits (in Cα trace) surrounding the quasi 3-fold axis nearest the icosahedral 2-fold were superimposed onto those surrounding the icosahedral 3-fold site. The figure is centered at the icosahedral 3-fold site. Rmsds in Cα were mapped onto the structure with different colors. Color scheme: blue, rmsd $\leq$ 1.5 Å; green, rmsd between 1.5 Å and 3.0 Å; yellow to red, rmsd > 3.0 Å. The icosahedral lattice is shown as yellow sticks.

(B) The phage L decoration protein density from the phage L versus the phage P22 difference map (Figure 3D) is superimposed above the X-ray structure of HK97. One asymmetric unit is shown as a ribbon diagram. The icosahedral lattice is shown as gold sticks. The icosahedral 5-, 3-, and 2-fold axes are indicated.

from that of the quasi 3-fold site close to the icosahedral 5-fold axis. The two decoration proteins of phage L must be capable of distinguishing the subtle difference between these two binding sites. This capability places the phage L decoration proteins into the same category as adenovirus polypeptide IX and phage ϕ29 head fibers, which are also able to discriminate between quasi equivalent sites (Morais et al., 2005; Saban et al., 2005; Stewart et al., 1993).

Homology between Dec and the Long Tail Fiber Proteins of a T4-like Phage

In an attempt to identify sequence and structural homology with other proteins, we performed a BLAST search (Altschul et al., 1997) with the Dec amino acid sequence. Interestingly, the search resulted in short but convincing

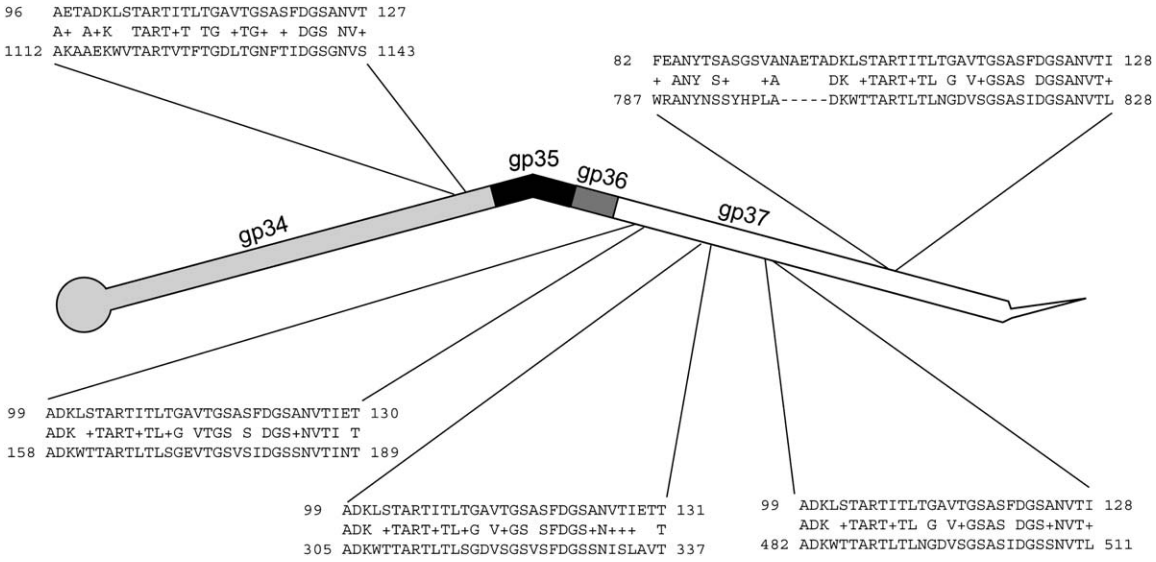

Figure 5. Sequence Similarity between the Phage L Dec Protein and the Long Tail Fiber Proteins of T4-like Phage KVP40

The tail fiber is drawn as a schematic diagram; the four component proteins, gp34–gp37, are labeled at relative positions. Regions of high sequence identity with Dec protein are indicated with blocks of sequence alignments. In each block, from the top, middle, and bottom lines are the Dec protein sequence, the identical residues, and the tail fiber sequence, respectively. Similar but not identical residues are indicated with a "+" in each middle line. The numbers of the first and last residues in each alignment are labeled.

matches between a block of ~30 carboxyl-proximal residues of Dec and segments from long tail fibers of several tailed phages (Figure 5). These include the long fibers of the T4-like vibriophage KVP40 and *Aeromonas salmonicida* phage 44RR2.8t (Miller et al., 2003; Tetart et al., 2001), as well as coliphage P1 (Lobocka et al., 2004) and *Pseudomonas aeruginosa* P2-like phage ϕCTX (Nakayama et al., 1999). In addition, similar homology is present in proteins homologous to phage T4 gp36 proteins that are present at the elbow of the T4 fiber. In particular, the highest similarity is for Dec residues 99–130 against residues 158–189 of the long tail fiber distal subunit of phage KVP40 with 71% identity and >90% similarity (Figure 5). This segment of KVP40 seems to define an important motif, as it appears four times in the sequence of the tail distal subunit and once in the proximal subunit of the long tail fiber. The functional implication of this similarity is 2-fold. First, in view of the trimeric status of Dec as well as all studied long tail fiber proteins (Cerritelli et al., 1996; Steven et al., 1988), and the fact that this motif is located in the distal domain (the knob) of Dec, it could contribute to Dec's trimerization. If so, the amino-proximal portion of Dec may form the leg of the tripod that makes contact with the major capsid protein. Second, it is also possible that the outward protruding portion of Dec protein carries additional function(s), as is known to be true of herpesvirus VP26 and adenovirus pIX decoration proteins (Douglas et al., 2004; Lutz et al., 1997; Rosa-Calatrava et al., 2001). Where they have been studied carefully, the long tail fibers of phages have been found to bind *reversibly* to abundant features on the surface of bacteria. It has been suggested that this allows the virions to "wander across the two-dimensional surface as tail fibers attach and detach at random, but would restrict them from rising off of the cell surface" in order to more efficiently find their true, irreversible cell surface receptor (Goldberg et al., 1994). Perhaps multiple protrusions extending from the phage head in the form of decoration proteins could perform a similar function, allowing the virion to more efficiently "search" a cell's surface for its true receptor without losing contact with the cell surface (one can even imagine short-tailed phages like phage L, which lack long tail fibers, "rolling" around on the surface of the bacterium). The similarity of the C-terminal Dec motif to phage tail fibers gives some speculative support for such a role.

Summary

A characteristic feature of virus capsid proteins is their capability of self-assembly into three-dimensional lattices with well-defined geometry. In many cases, this is achieved by a single capsid protein. In some cases, this is accompanied by one or more decoration protein. These decoration proteins are either dispensable for capsid assembly, or they are required for capsid stability; in the later case, these proteins are called molecular cement or glue. We have identified and structurally characterized two cementing proteins in dsDNA bacteriophage L. One of them, the Dec, binds at the quasi 3-fold axes nearest the icosahedral 2-fold axes, and the other binds at the icosahedral 3-fold vertices, both in a homotrimeric form. None of them binds at the quasi 6-fold axis of the canonical hexamer or at the quasi 3-fold axes in close proximity to the icosahedral 5-fold vertices. These data indicate discriminatory recognition of the two cementing proteins upon only a subset of the quasi equivalent sites on the phage capsid. An atomic structure of the phage L will be needed to elucidate the molecular basis underlying this discriminatory binding of cementing proteins to sites with only subtle structural differences, and it will help us understand the self-assembly in large, complex systems.

Table 1. Statistics of Image Reconstructions

	Number of Particles	Defocus Range, μm	Resolution, Å
Phage L	5581	0.6–2.7	15
Phage P22 virions	1933	0.8–3.0	18
Phage P22 + Dec	1391	0.6–3.0	29

Experimental Procedures

Preparation of Phages and Proteins

Preparation of phages L *cII*$^-$ and P22 *c1*$^-$7 *13*$^-$*am*H101 virions, expression, purification of phage L Dec protein, and decoration of phage P22 with Dec protein were performed as described (an excess of purified protein was mixed with purified P22 virions at room temperature for 30 min in 1 mM $MgCl_2$, 10 mM Tris-HCl [pH 7.4], and the modified virions were purified from unassembled Dec protein by CsCl step gradient centrifugation [Gilcrease et al., 2005]). Phages were propagated on *Salmonella enterica* serovar Typhimurium strain DB7000 (Winston et al., 1979) and purified as described by CsCl density centrifugation (Casjens and Hayden, 1988). The phage L gene *Dec* was cloned into pET-21b vector (Invitrogen) with a carboxyl hexahistidine tag and expressed in *E. coli* strain BL21(DE3) pLysS, and the protein was purified over an Ni-NTA column (Qiagen) (Gilcrease et al., 2005).

Electron Cryo-Microscopy and Three-Dimensional Reconstruction

The sample was frozen-hydrated in vitrified ice on holey EM grids by following a standard procedure (Adrian et al., 1984; van Heel et al., 2000). Briefly, 5 μl of sample was applied for 1 min onto a copper grid previously glow discharged and coated with a holey carbon film. The grid was blotted with Whatman #2 filter paper, plunged into a slush of liquid ethane, and stored in liquid nitrogen. The grid was transferred with a Gatan 626 cryostage (Gatan, Inc., Pleasanton, CA) into a Phillips CM200FEG transmission electron microscope (Philips/FEI, Eindhoven, The Netherlands) operated at an accelerating voltage of 200 kV. Electron micrographs were recorded at a magnification of 38,000 on Kodak SO156 film under low-dose conditions (5–20 electrons/Å^2). Micrographs were digitized by using a Zeiss SCAI scanner (Z/I Imaging Corporation, Madison, AL) with a step size of 7 μm, and then averaged to a pixel size of 3.684 Å. Particles were boxed into a 300 × 300 dimension with the program EMAN (Ludtke et al., 1999), and image reconstruction was carried out with the program SPIDER (Frank et al., 1996). The contrast transfer function was corrected by phase flipping over the boxed particles. The resolution was estimated with the Fourier shell correlation method (van Heel et al., 2000). Statistics of the reconstructions are listed in Table 1. Isosurface rendition of the reconstructions was performed with the program Chimera (Pettersen et al., 2004).

Difference Map

Difference maps were calculated as follows: Maps were first low-pass filtered to the lower resolution of each pair. When calculating the difference map between phage L and wild-type phage P22, the phage L map was filtered to 18 Å. When calculating the difference map between phage P22 plus Dec and wild-type phage P22, the wild-type phage P22 map was filtered to 29 Å. Two schemes for density scaling were used. In the first scheme, the two maps were linearly scaled so that they had the same maximal and minimal densities for the capsid shell, which is between radii 376 and 273 Å. In the second scheme, each map was normalized so that the average density was set to zero and the density value equaled the number of standard deviations above the average density. The two schemes yielded virtually identical results. The difference maps presented in the text were calculated with the first method. All maps were contoured at a density level that resulted in a volume corresponding to 100% of the expected molecular mass of coat protein or decoration protein, assuming the protein density to be 1.34 mg/ml. In the cryo-EM maps of the phage L virion and the difference map between phages L and P22, the molecular mass of ORF129 was used as an estimate for that of the second decoration protein, as this second decoration protein hasn't been genetically identified.

Acknowledgments

This work was supported by National Institutes of Health grant AI40101 to J.E.J. and National Science Foundation grant MCB-990526 to S.R.C.

Received: January 26, 2006
Revised: February 28, 2006
Accepted: March 1, 2006
Published: May 16, 2006

References

Adrian, M., Dubochet, J., Lepault, J., and McDowall, A.W. (1984). Cryo-electron microscopy of viruses. Nature *308*, 32–36.

Altschul, S.F., Madden, T.L., Schaffer, A.A., Zhang, J., Zhang, Z., Miller, W., and Lipman, D.J. (1997). Gapped BLAST and PSI-BLAST: a new generation of protein database search programs. Nucleic Acids Res. *25*, 3389–3402.

Booy, F.P., Newcomb, W.W., Trus, B.L., Brown, J.C., Baker, T.S., and Steven, A.C. (1991). Liquid-crystalline, phage-like packing of encapsidated DNA in herpes simplex virus. Cell *64*, 1007–1015.

Casjens, S. (1979). Molecular organization of the bacteriophage P22 coat protein shell. J. Mol. Biol. *131*, 1–14.

Casjens, S., and Hayden, M. (1988). Analysis *in vivo* of the bacteriophage P22 headful nuclease. J. Mol. Biol. *199*, 467–474.

Casjens, S., and Hendrix, R. (1988). Control mechanisms in dsDNA bacteriophage assembly. In The Bacteriophages, R. Calendar, ed. (New York City: Plenum Press), pp. 15–91.

Casjens, S.R., and Hendrix, R.W. (1974). Locations and amounts of major structural proteins in bacteriophage λ. J. Mol. Biol. *88*, 535–545.

Caspar, D., and Klug, A. (1962). Physical principles in the construction of regular viruses. Cold Spring Harb. Symp. Quant. Biol. *27*, 1–27.

Cerritelli, M.E., Wall, J.S., Simon, M.N., Conway, J.F., and Steven, A.C. (1996). Stoichiometry and domainal organization of the long tail-fiber of bacteriophage T4: a hinged viral adhesin. J. Mol. Biol. *260*, 767–780.

Cerritelli, M.E., Cheng, N., Rosenberg, A.H., McPherson, C.E., Booy, F.P., and Steven, A.C. (1997). Encapsidated conformation of bacteriophage T7 DNA. Cell *91*, 271–280.

Dokland, T., and Murialdo, H. (1993). Structural transitions during maturation of bacteriophage λ capsids. J. Mol. Biol. *233*, 682–694.

Douglas, M.W., Diefenbach, R.J., Homa, F.L., Miranda-Saksena, M., Rixon, F.J., Vittone, V., Byth, K., and Cunningham, A.L. (2004). Herpes simplex virus type 1 capsid protein VP26 interacts with dynein light chains RP3 and Tctex1 and plays a role in retrograde cellular transport. J. Biol. Chem. *279*, 28522–28530.

Earnshaw, W.C., and Harrison, S.C. (1977). DNA arrangement in isometric phage heads. Nature *268*, 598–602.

Earnshaw, W., Casjens, S., and Harrison, S. (1976). Assembly of the head of bacteriophage P22, X-ray diffraction from heads, proheads and related structures. J. Mol. Biol. *104*, 387–410.

Fabry, C.M., Rosa-Calatrava, M., Conway, J.F., Zubieta, C., Cusack, S., Ruigrok, R.W., and Schoehn, G. (2005). A quasi-atomic model of human adenovirus type 5 capsid. EMBO J. *24*, 1645–1654.

Fokine, A., Chipman, P.R., Leiman, P.G., Mesyanzhinov, V.V., Rao, V.B., and Rossmann, M.G. (2004). Molecular architecture of the prolate head of bacteriophage T4. Proc. Natl. Acad. Sci. USA *101*, 6003–6008.

Fokine, A., Kostyuchenko, V.A., Efimov, A.V., Kurochkina, L.P., Sykilinda, N.N., Robben, J., Volckaert, G., Hoenger, A., Chipman, P.R., Battisti, A.J., et al. (2005). A three-dimensional cryo-electron microscopy structure of the bacteriophage phiKZ head. J. Mol. Biol. *352*, 117–124.

Frank, J., Radermacher, M., Penczek, P., Li, Y., and Ladjadj, M. (1996). SPIDER and WEB: processing and visualization of images in 3D electron microscopy and related fields. J. Struct. Biol. *116*, 190–199.

Furcinitti, P.S., van Oostrum, J., and Burnett, R.M. (1989). Adenovirus polypeptide IX revealed as capsid cement by difference images from electron microscopy and crystallography. EMBO J. *8*, 3563–3570.

Gilcrease, E., Winn-Stapley, D., Hewitt, F., Joss, L., and Casjens, S. (2005). Nucleotide sequence of the head assembly gene cluster of bacteriophage L and decoration protein characterization. J. Bacteriol. *187*, 2050–2057.

Goldberg, E., Grinius, L., and Leterllier, L. (1994). Recognition, attachement and injection. In The Molecular Biology of Bacteriophage T4, J. Karam, ed. (Washington, DC: ASM press), pp. 347–356.

Gupta, A., Onda, M., Pastan, I., Adhya, S., and Chaudhary, V.K. (2003). High-density functional display of proteins on bacteriophage λ. J. Mol. Biol. *334*, 241–254.

Hayden, M., Adams, M.B., and Casjens, S. (1985). Bacteriophage L: chromosome physical map and structural proteins. Virology *147*, 431–440.

Imber, R., Tsugita, A., Wurtz, M., and Hohn, T. (1980). Outer surface protein of bacteriophage λ. J. Mol. Biol. *139*, 277–295.

Ishii, T., and Yanagida, M. (1977). The two dispensable structural proteins (soc and hoc) of the T4 phage capsid; their purification and properties, isolation and characterization of the defective mutants, and their binding with the defective heads in vitro. J. Mol. Biol. *109*, 487–514.

Iwasaki, K., Trus, B.L., Wingfield, P.T., Cheng, N., Campusano, G., Rao, V.B., and Steven, A.C. (2000). Molecular architecture of bacteriophage T4 capsid: vertex structure and bimodal binding of the stabilizing accessory protein. Soc. Virology *271*, 321–333.

Jiang, W., Li, Z., Zhang, Z., Baker, M.L., Prevelige, P.E., Jr., and Chiu, W. (2003). Coat protein fold and maturation transition of bacteriophage P22 seen at subnanometer resolutions. Nat. Struct. Biol. *10*, 131–135.

Kang, S., and Prevelige, P.E., Jr. (2005). Domain study of bacteriophage p22 coat protein and characterization of the capsid lattice transformation by hydrogen/deuterium exchange. J. Mol. Biol. *347*, 935–948.

Lobocka, M.B., Rose, D.J., Plunkett, G., 3rd, Rusin, M., Samojedny, A., Lehnherr, H., Yarmolinsky, M.B., and Blattner, F.R. (2004). Genome of bacteriophage P1. J. Bacteriol. *186*, 7032–7068.

Ludtke, S.J., Baldwin, P.R., and Chiu, W. (1999). EMAN: semiautomated software for high-resolution single-particle reconstructions. J. Struct. Biol. *128*, 82–97.

Lutz, P., Rosa-Calatrava, M., and Kedinger, C. (1997). The product of the adenovirus intermediate gene IX is a transcriptional activator. J. Virol. *71*, 5102–5109.

Meulenbroek, R.A., Sargent, K.L., Lunde, J., Jasmin, B.J., and Parks, R.J. (2004). Use of adenovirus protein IX (pIX) to display large polypeptides on the virion—generation of fluorescent virus through the incorporation of pIX-GFP. Mol. Ther. *9*, 617–624.

Mikawa, Y., Maruyama, I., and Brenner, S. (1996). Surface display of proteins on bacteriophage λ heads. J. Mol. Biol. *262*, 21–30.

Miller, E.S., Heidelberg, J.F., Eisen, J.A., Nelson, W.C., Durkin, A.S., Ciecko, A., Feldblyum, T.V., White, O., Paulsen, I.T., Nierman, W.C., et al. (2003). Complete genome sequence of the broad-host-range vibriophage KVP40: comparative genomics of a T4-related bacteriophage. J. Bacteriol. *185*, 5220–5233.

Mmolawa, P.T., Schmieger, H., Tucker, C.P., and Heuzenroeder, M.W. (2003). Genomic structure of the *Salmonella enterica* serovar Typhimurium DT 64 bacteriophage ST64T: evidence for modular genetic architecture. J. Bacteriol. *185*, 3473–3475.

Morais, M.C., Choi, K.H., Koti, J.S., Chipman, P.R., Anderson, D.L., and Rossmann, M.G. (2005). Conservation of the capsid structure in tailed dsDNA bacteriophages: the pseudoatomic structure of phi29. Mol. Cell *18*, 149–159.

Nakayama, K., Kanaya, S., Ohnishi, M., Terawaki, Y., and Hayashi, T. (1999). The complete nucleotide sequence of fCTX, a cytotoxin-converting phage of *Pseudomonas aeruginosa*: implications for phage evolution and horizontal gene transfer via bacteriophages. Mol. Microbiol. *31*, 399–419.

Newcomb, W.W., Trus, B.L., Booy, F.P., Steven, A.C., Wall, J.S., and Brown, J.C. (1993). Structure of the herpes simplex virus capsid. Molecular composition of the pentons and the triplexes. J. Mol. Biol. *232*, 499–511.

Newcomb, W.W., Trus, B.L., Cheng, N., Steven, A.C., Sheaffer, A.K., Tenney, D.J., Weller, S.K., and Brown, J.C. (2000). Isolation of herpes simplex virus procapsids from cells infected with a protease-deficient mutant virus. J. Virol. *74*, 1663–1673.

Pettersen, E.F., Goddard, T.D., Huang, C.C., Couch, G.S., Greenblatt, D.M., Meng, E.C., and Ferrin, T.E. (2004). UCSF Chimera—a visualization system for exploratory research and analysis. J. Comput. Chem. *25*, 1605–1612.

Prasad, B.V., Prevelige, P.E., Marietta, E., Chen, R.O., Thomas, D., King, J., and Chiu, W. (1993). Three-dimensional transformation of capsids associated with genome packaging in a bacterial virus. J. Mol. Biol. *231*, 65–74.

Prevelige, P.E., Jr. (2005). Bacteriophage P22. In The Bacteriophages, Second Edition, R. Calendar, ed. (Oxford, UK: Oxford University Press), pp. 457–468.

Rosa-Calatrava, M., Grave, L., Puvion-Dutilleul, F., Chatton, B., and Kedinger, C. (2001). Functional analysis of adenovirus protein IX identifies domains involved in capsid stability, transcriptional activity, and nuclear reorganization. J. Virol. *75*, 7131–7141.

Rux, J.J., and Burnett, R.M. (2004). Adenovirus structure. Hum. Gene Ther. *15*, 1167–1176.

Saad, A., Zhou, Z.H., Jakana, J., Chiu, W., and Rixon, F.J. (1999). Roles of triplex and scaffolding proteins in herpes simplex virus type 1 capsid formation suggested by structures of recombinant particles. J. Virol. *73*, 6821–6830.

Saban, S.D., Nepomuceno, R.R., Gritton, L.D., Nemerow, G.R., and Stewart, P.L. (2005). Cryo-EM structure at 9 Å resolution of an adenovirus vector targeted to hematopoietic cells. J. Mol. Biol. *349*, 526–537.

San Martin, C., Huiskonen, J.T., Bamford, J.K., Butcher, S.J., Fuller, S.D., Bamford, D.H., and Burnett, R.M. (2002). Minor proteins, mobile arms and membrane-capsid interactions in the bacteriophage PRD1 capsid. Nat. Struct. Biol. *9*, 756–763.

Sargent, K.L., Ng, P., Evelegh, C., Graham, F.L., and Parks, R.J. (2004). Development of a size-restricted pIX-deleted helper virus for amplification of helper-dependent adenovirus vectors. Gene Ther. *11*, 504–511.

Spencer, J.V., Newcomb, W.W., Thomsen, D.R., Homa, F.L., and Brown, J.C. (1998). Assembly of the herpes simplex virus capsid: preformed triplexes bind to the nascent capsid. J. Virol. *72*, 3944–3951.

Sternberg, N., and Weisberg, R. (1977). Packaging of coliphage λ DNA. II. The role of the gene D protein. J. Mol. Biol. *117*, 733–759.

Steven, A.C., Trus, B.L., Maizel, J.V., Unser, M., Parry, D.A., Wall, J.S., Hainfeld, J.F., and Studier, F.W. (1988). Molecular substructure of a viral receptor-recognition protein. The gp17 tail-fiber of bacteriophage T7. J. Mol. Biol. *200*, 351–365.

Steven, A.C., Greenstone, H.L., Booy, F.P., Black, L.W., and Ross, P.D. (1992). Conformational changes of a viral capsid protein. Thermodynamic rationale for proteolytic regulation of bacteriophage T4 capsid expansion, co-operativity, and super-stabilization by soc binding. J. Mol. Biol. *228*, 870–884.

Stewart, P.L., Burnett, R.M., Cyrklaff, M., and Fuller, S.D. (1991). Image reconstruction reveals the complex molecular organization of adenovirus. Cell *67*, 145–154.

Stewart, P.L., Fuller, S.D., and Burnett, R.M. (1993). Difference imaging of adenovirus: bridging the resolution gap between X-ray crystallography and electron microscopy. EMBO J. *12*, 2589–2599.

Tao, Y., Olson, N.H., Xu, W., Anderson, D.L., Rossmann, M.G., and Baker, T.S. (1998). Assembly of a tailed bacterial virus and its genome release studied in three dimensions. Cell *95*, 431–437.

Tetart, F., Desplats, C., Kutateladze, M., Monod, C., Ackermann, H.W., and Krisch, H.M. (2001). Phylogeny of the major head and tail genes of the wide-ranging T4-type bacteriophages. J. Bacteriol. *183*, 358–366.

Trus, B.L., Homa, F.L., Booy, F.P., Newcomb, W.W., Thomsen, D.R., Cheng, N., Brown, J.C., and Steven, A.C. (1995). Herpes simplex virus capsids assembled in insect cells infected with recombinant baculoviruses: structural authenticity and localization of VP26. J. Virol. *69*, 7362–7366.

van Heel, M., Gowen, B., Matadeen, R., Orlova, E., Finn, R., Pape, T., Cohen, D., Stark, H., Schmidt, R., Schatz, M., and Patwardhan, A. (2000). Single-particle electron cryo-microscopy: towards atomic resolution. Q. Rev. Biophys. *33*, 307–369.

Vellinga, J., Van der Heijdt, S., and Hoeben, R.C. (2005). The adenovirus capsid: major progress in minor proteins. J. Gen. Virol. *86*, 1581–1588.

Wendt, J.L., and Feiss, M. (2004). A fragile lattice: replacing bacteriophage λ's head stability gene D with the shp gene of phage 21 generates the Mg2+-dependent virus, λ shp. Virology *326*, 41–46.

Wikoff, W.R., Liljas, L., Duda, R.L., Tsuruta, H., Hendrix, R.W., and Johnson, J.E. (2000). Topologically linked protein rings in the bacteriophage HK97 capsid. Science *289*, 2129–2133.

Winston, F., Botstein, D., and Miller, J.H. (1979). Characterization of amber and ochre suppressors in *Salmonella typhimurium*. J. Bacteriol. *137*, 433–439.

Yanagida, M. (1977). Molecular organization of the shell of T-even bacteriophage head. II. Arrangement of subunits in the head shell of giant phages. J. Mol. Biol. *109*, 515–537.

Yanagida, M., Suzuki, Y., and Toda, T. (1984). Molecular organization of the head of bacteriophage Teven: underlying design principles. Adv. Biophys. *17*, 97–146.

Zakhartchouk, A., Connors, W., van Kessel, A., and Tikoo, S.K. (2004). Bovine adenovirus type 3 containing heterologous protein in the C-terminus of minor capsid protein IX. Virology *320*, 291–300.

Zhang, Z., Greene, B., Thuman-Commike, P.A., Jakana, J., Prevelige, P.E., Jr., King, J., and Chiu, W. (2000). Visualization of the maturation transition in bacteriophage P22 by electron cryomicroscopy. J. Mol. Biol. *297*, 615–626.

Zhou, Z.H., He, J., Jakana, J., Tatman, J.D., Rixon, F.J., and Chiu, W. (1995). Assembly of VP26 in herpes simplex virus-1 inferred from structures of wild-type and recombinant capsids. Nat. Struct. Biol. *2*, 1026–1030.

Zhou, Z.H., Chen, D.H., Jakana, J., Rixon, F.J., and Chiu, W. (1999). Visualization of tegument-capsid interactions and DNA in intact herpes simplex virus type 1 virions. J. Virol. *73*, 3210–3218.